iScience

Article

Genomic characteristics of emerging human pathogen *Rickettsia aeschlimannii* isolated from two *Hyalomma* tick species

Graphical abstract

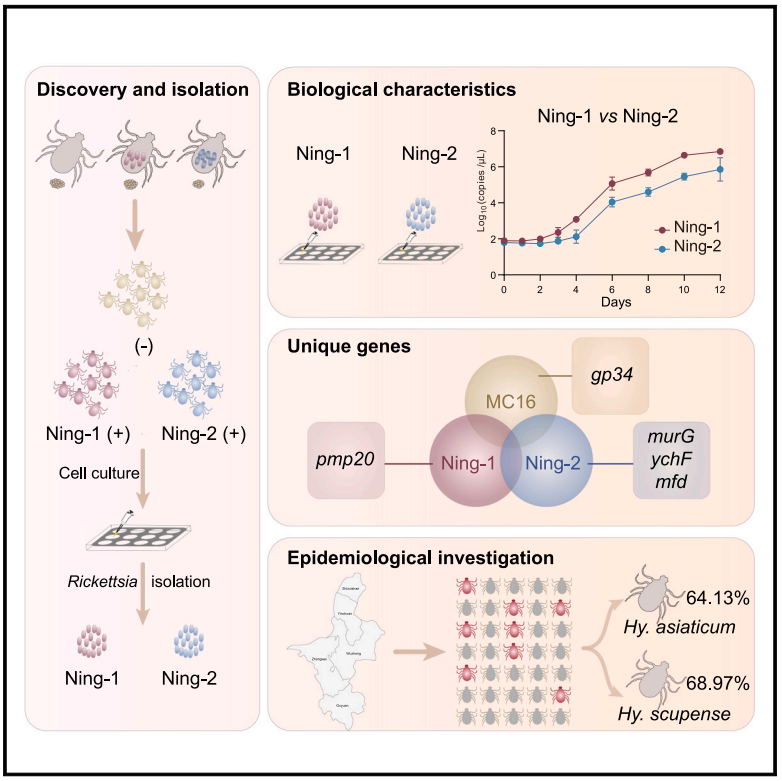

Highlights

- Two *R. aeschlimannii* strains were isolated from two species of *Hyalomma* ticks
- Two Chinese isolates show genomic features distinct from Mediterranean isolate
- One rickettsial isolate grows faster in cell culture than another
- *R. aeschlimannii* is highly prevalent among *Hyalomma* ticks in Ningxia, China

Authors

Ning Wang, Run-Ze Ye, Hui-Jun Yu, ..., Xiao-Ming Cui, Zhi-Hong Liu, Wu-Chun Cao

Correspondence

cuixm7@163.com (X.-M.C.), jwclzh@163.com (Z.-H.L.), caowuchun@126.com (W.-C.C.)

In brief

Genomics; Pathogenic organism

Wang et al., 2025, iScience *28*, 112080
March 21, 2025
https://doi.org/10.1016/j.isci.2025.112080

CellPress

iScience

CellPress
OPEN ACCESS

Article

Genomic characteristics of emerging human pathogen *Rickettsia aeschlimannii* isolated from two *Hyalomma* tick species

Ning Wang,[1,2] Run-Ze Ye,[4] Hui-Jun Yu,[1] Xiao-Yu Han,[2] Di Tian,[3] Wan-Ying Gao,[1] Bai-Hui Wang,[1] Li-Feng Du,[1] Ming-Zhu Zhang,[1] Xiao-Yu Shi,[2] Dai-Yun Zhu,[2] Wenqiang Shi,[2] Na Jia,[2] Jia-Fu Jiang,[2] Yi Sun,[2] Lin Zhao,[1] Xiao-Ming Cui,[2,5,*] Zhi-Hong Liu,[3,*] and Wu-Chun Cao[1,2,5,6,*]

[1]Institute of EcoHealth, School of Public Health, Cheeloo College of Medicine, Shandong University, Jinan, Shandong 250012, China
[2]State Key Laboratory of Pathogen and Biosecurity, AMMS, Beijing 100071, China
[3]School of Public Health, Ningxia Medical University, Yinchuan, Ningxia 750000, China
[4]Department of Emergency Medicine, Qilu Hospital of Shandong University, Jinan, Shandong 250012, China
[5]Research Unit of Discovery and Tracing of Natural Focus Diseases, Chinese Academy of Medical Sciences, Beijing 100071, China
[6]Lead contact
*Correspondence: cuixm7@163.com (X.-M.C.), jwclzh@163.com (Z.-H.L.), caowuchun@126.com (W.-C.C.)
https://doi.org/10.1016/j.isci.2025.112080

SUMMARY

Rickettsia aeschlimannii, which emerged in Morocco in 1997, causes the Mediterranean spotted fever-like rickettsiosis in various Mediterranean countries and recently in Russia and China. Despite its increasing distribution, no available genome has been reported outside Morocco to date. Here, we isolated two strains of *R. aeschlimannii* from *Hyalomma asiaticum* (Ning-1 strain) and *Hyalomma scupense* (Ning-2 strain) ticks in northwestern China and assembled their complete genomes. The genomes of the two strains were smaller than the Mediterranean MC16 strain, containing fewer pseudogenes, higher *ralF* virulence factor coverage, and 154 unique orthogroups. The Ning-1 strain overwhelmed the Ning-2 strain with more obvious cytopathic effects, quicker growth, and faster plaque formation in cell culture, likely due to its unique *pmp20* gene, higher frequency of single nucleotide polymorphisms, and missense/silent ratio. The prevalence of *R. aeschlimannii* was high among *Hyalomma* ticks in northwestern China. These findings highlight the genomic characteristics of *R. aeschlimannii* and the necessity for enhanced surveillance of the emerging *Rickettsia* in the human population.

INTRODUCTION

Rickettsia aeschlimannii, a member of the spotted fever group rickettsiae (SFGR), was identified in *Hyalomma marginatum* ticks in Morocco in 1997.[1] After five years, a human case of *R. aeschlimannii* infection was reported in France in 2002, which can cause a Mediterranean spotted fever (MSF)-like rickettsiosis.[2,3] Subsequent cases have been reported in other Mediterranean countries, including Greece,[4] Algeria,[5,6] and Italy.[7] Patients infected with *R. aeschlimannii* exhibit symptoms, such as fever, headache, myalgia, vomiting, rash, eschars, papules, necrosis at the tick bite site, and may also experience liver dysfunction.[2,5,7] In 2022, cases of *R. aeschlimannii* infection were reported outside the Mediterranean region, in Russia and Xinjiang, China.[8,9] The increasing number of infections and the expanding geographic distribution of this emerging pathogen highlight the need for enhanced surveillance and public health awareness.

In addition to *Hyalomma*,[10–12] *R. aeschlimannii* has also been detected in various tick species, including *Rhipicephalus*,[13–15] *Dermacentor*,[16] as well as *Ixodes* and *Haemaphysalis* tick species.[17–19] *R. aeschlimannii* can be transovarially transmitted in *Hy. marginatum* and detected in both engorged females and their larvae,[20] increasing the likelihood of tick-borne transmission to humans. Currently, only one isolate of *R. aeschlimannii* from *Hy. marginatum* in Morocco has been sequenced,[1] providing a draft genome sequence.[21] This limits our ability to compare genetic characteristics of this *Rickettsia* across different regions and tick species, thereby hindering our understanding of its pathogenic mechanisms.

In this study, we obtained two isolates of *R. aeschlimannii* from *Hyalomma asiaticum* and *Hyalomma scupense* ticks in China and assembled their whole-genome sequences using next-generation sequencing. We performed genomic analyses in comparison with the Mediterranean isolate and estimated the infection rate of *R. aeschlimannii* in *Hyalomma* ticks in potential risk areas.

RESULTS

Discovery of *Rickettsia aeschlimannii* isolates from two *Hyalomma* species

In 2022, we collected engorged *Hy. scupense* and *Hy. asiaticum* female ticks from goats in Pingluo County and Zhongning

County, Ningxia, China. Under laboratory conditions, these engorged female ticks laid eggs that subsequently hatched into larvae. Approximately one hundred larvae of each species were ground separately into two pools. The supernatants were inoculated into African green monkey kidney (Vero 81) cells. Simultaneously, DNA was extracted from the supernatant of both pools, and SFGR-specific *ompA* and *gltA* genes (Table S1) were amplified and confirmed using Sanger sequencing. The *ompA* gene sequences were 100% identical (603/603) to that of the *R. aeschlimannii* isolate Baiyin-Ha-14 reported from *Hy. asiaticum* in Gansu, China (GenBank: MH932058). The *gltA* gene sequences showed 100% identity (636/636) and 99.84% identity (635/636) with the sequences of *R. aeschlimannii* isolate Baiyin-Hm-256 from *Hy. marginatum* in Gansu, China (GenBank: MH932015), suggesting the possible presence of two strains of *R. aeschlimannii*. Four weeks post-inoculation, rickettsial bacilli were observed using Giemsa staining, exhibiting small purple-colored coccobacillus morphology (Figures 1A and 1B). Transmission electron micrographs showed *Rickettsia* scattered in the cytoplasm, rod-shaped or coccoid, with sizes around 0.5–1.2 μm in length and 0.3–0.5 μm in width (Figures 1C and 1D).

Genomic and phylogenetic analysis of two *Rickettsia aeschlimannii* strains

DNA was extracted from purified bacteria cultured in Vero 81 cells. Using next-generation sequencing and *de novo* assembly, we obtained two complete genome sequences of *R. aeschlimannii* from two different tick species, which exhibited variations in genome size. Comparative genomic analysis (Figures 2A and 2B; Table 1) indicated that the genomes of two *R. aeschlimannii* isolates were smaller than that of the Mediterranean strain MC16 (GenBank: GCA_001051325.1). Although the GC content, number of rRNAs, and tRNAs were consistent among the three *R. aeschlimannii* strains, the two strains obtained in this study harbored fewer genes, coding sequences, and pseudogenes compared to the strain MC16 (Table 1). The phylogenetic tree based on whole genomes showed that the two strains clustered with *R. aeschlimannii* str MC16 (Figure 2C) and shared average nucleotide identity (ANI) of 99.90% and 99.89% with strain MC16 (Figure S1). The ANI between the two newly characterized strains was 99.98%. The genome sequences were designated as *R. aeschlimannii* strain Ning-1 (isolated from *Hy. asiaticum*) and *R. aeschlimannii* strain Ning-2 (isolated from *Hy. scupense*), and have been submitted to GenBank with the accession numbers JBFQGP000000000 and JBFQGO000000000.

Biological characteristics of two *Rickettsia aeschlimannii* isolates

Vero 81 cells and *Ixodes scapularis* tick cell line (IDE8 cells) were infected with *R. aeschlimannii* str. Ning-1 (Ning-1 strain) and *R. aeschlimannii* str. Ning-2 (Ning-2 strain). According to the growth curve (Figure 3A), both isolates exhibited three growth phases in Vero 81 and IDE8 cells: the lag phase (0–2 days), the exponential phase (3–8 days), and the stationary phase (9–12 days). However, the Ning-1 strain showed a significantly higher bacterial load than the Ning-2 strain in both Vero 81 and IDE8 cells at identical inoculum concentrations during the exponential phase and stationary phases, indicating that the Ning-1 strain had a higher growth rate and greater adaptability.

To assess their virulence differences, we compared cytopathic effects (CPE) of the two *R. aeschlimannii* strains on Vero 81 cells. At the same inoculum concentration, the Ning-1 strain induced noticeable CPE by day 4 (Figure 3B), whereas cells infected with the Ning-2 strain did not show significant effects. Throughout the observation period, the Ning-1 strain exhibited a stronger CPE. The plaque assay results (Figure 3C) revealed that, at the same concentration, the Ning-2 strain exhibited delayed plaque formation compared to the Ning-1 strain. By day 8, at a 10^{-4} dilution, the Ning-1 strain formed more obvious plaques than the Ning-2 strain. In cell culture infection models, the Ning-1 strain overwhelmed the Ning-2 strain with more obvious CPE, quicker growth, and faster plaque formation.

Comparison of genome annotation among *Rickettsia aeschlimannii* strains

To further investigate the potential factors causing the biological differences between the two isolates, we compared their genomic characteristics and homologous genes. The similarities and differences among the three *R. aeschlimannii* strains and other closely related representative strains (Figure 4A) revealed that the three *R. aeschlimannii* strains shared 821 orthogroups with other SFGRs but possessed 42 orthogroups unique to them that were absent in other SFGRs. Notably, strains Ning-1, Ning-2, and MC16 each possessed three, five, and 25 unique orthogroups, respectively. Additionally, Ning-1 and Ning-2 shared 154 orthogroups not present in the MC16 genome.

We then annotated all the genes of three *R. aeschlimannii* strains using the clusters of orthologous groups of proteins (COG) databases to understand the differences in gene function. The three *R. aeschlimannii* strains had the highest number of proteins in three categories: S (function unknown), J (translation, ribosomal structure, and biogenesis), and M (cell wall/membrane/envelope biogenesis) (Figure 4B; Table S2). Except for categories A (RNA processing and modification) and Q (secondary metabolites biosynthesis, transport, and catabolism), the two *R. aeschlimannii* strains from this study possessed more proteins in all other categories than the Mediterranean MC16 strain.

Among the 154 orthogroups shared by the strains Ning-1 and Ning-2 (Figure 4C), 43 homologous genes were primarily annotated to categories related to transport and metabolism (categories E, P, and G), DNA replication, repair, and recombination (category L), and signal transduction (category T). Eighteen homologous genes were annotated as category S (function unknown), and the remaining genes were unannotated in the COG database. These findings suggest that the Ning-1 and Ning-2 strains may possess distinct characteristics or adaptations compared to the MC16 strain, which could affect their survival strategies and physiological functions.

Among the unique homologous genes of the three *R. aeschlimannii* strains, two genes of the Ning-1 strain were annotated as categories O (posttranslational modification, protein turnover, and chaperones) and U (intracellular trafficking, secretion, and vesicular transport) (Table S3). Three genes of the Ning-2 strain were annotated as categories M (cell

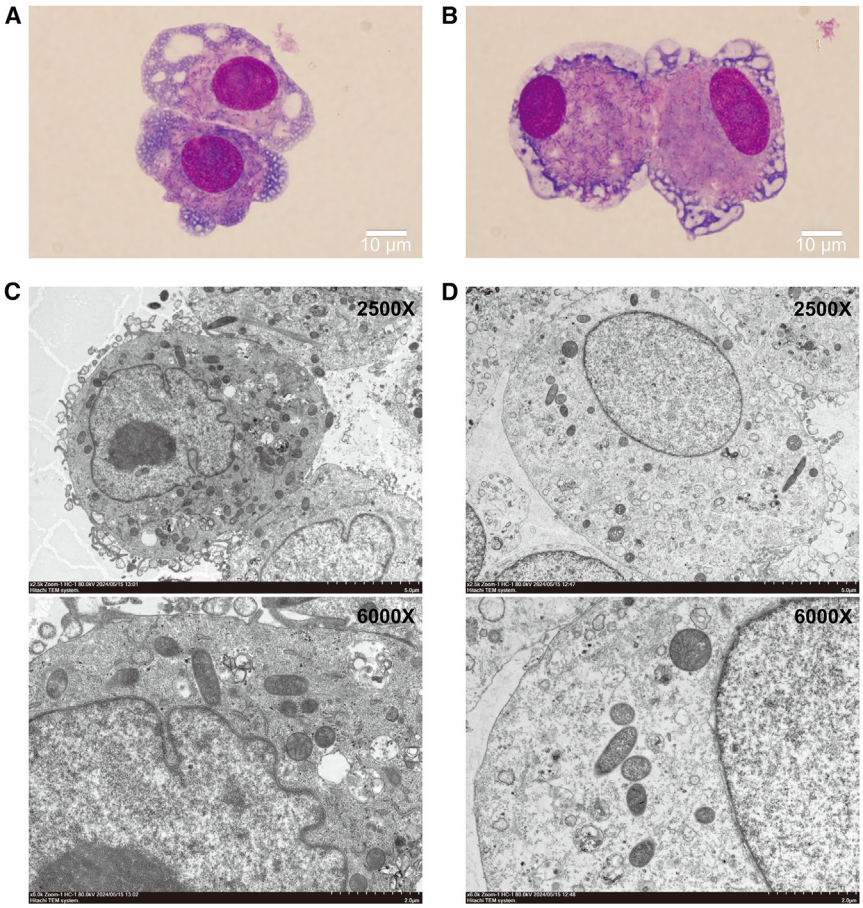

Figure 1. Isolation of *R. aeschlimannii* from two *Hyalomma* species

(A) Giemsa staining of *R. aeschlimannii* isolated from a pool of *Hy. asiaticum* larvae in Vero 81 cells.

(B) Giemsa staining of *R. aeschlimannii* isolated from a pool of *Hy. scupense* larvae in Vero 81 cells. Scale bar represents 10 μm (A and B).

(C) Transmission electron micrographs of Vero 81 cells infected with *R. aeschlimannii* isolated from *Hy. asiaticum*.

(D) Transmission electron micrographs of Vero 81 cells infected with *R. aeschlimannii* isolated from *Hy. scupense*. Photomicrographs were captured with an HT7800 transmission electron microscope camera. Scale bar represents 5 μm (magnification ×2,500) and 2 μm (magnification ×6,000) (C and D).

wall/membrane/envelope biogenesis), J (translation, ribosomal structure, and biogenesis), and L (replication, recombination, and repair). For the MC16 strain, only three genes were annotated as categories L (replication, recombination, and repair), I (lipid transport and metabolism), and N (cell motility). Apart from these, the remaining unique genes of the three *R. aeschlimannii* strains were unannotated. Notably, the Ning-1 strain possesses a unique orthologous group containing only one homologous gene (*pmp20*) in the U class, suggesting enhanced intracellular trafficking functions compared to the other two strains, which may improve its growth and replication capabilities in host cells, thereby contributing to its higher virulence.[22,23]

Virulence genes and single nucleotide polymorphism of *Rickettsia aeschlimannii*

All eight types of virulence genes were identified in the three *R. aeschlimannii* strains (Figure 5A). Notably, the Ning-1 and Ning-2 strains exhibited higher coverage of the *ralF* protein compared to the MC16 strain, suggesting potentially greater virulence. The *ralF* protein, an effector of the type IV secretion system (T4SS) with a Sec7 domain, modulates various host cell processes and facilitates the successful invasion, survival, and replication of *Rickettsia* within host cells.[24]

For the Ning-1 strain, the counts of variants, deletions, transitions, and transversions were 929, 46, 625, and 203, respectively, which were all higher than those in the Ning-2 strain (775, 27, 541, and 165) (Figure 5B; Table S4). The functional impacts of most single nucleotide polymorphisms (SNPs) were classified as modifier (Table S5) and typically occurred in non-coding regions or regions without known functions. There were 10,907 and 9,081 SNPs classified as modifier, accounting for 94.21% and 94.08% of the total SNPs in the strains Ning-1 and Ning-2, respectively. The numbers of variants with high, medium, and low impacts on protein structure, function, or stability were 63, 342, and 266 for the Ning-1 strain, and 48, 286, and 237 for the Ning-2 strain, respectively. Based on the impact of these variations on amino acid molecules, the mutations can be categorized as missense, nonsense, and silent mutations. The missense/silent ratio in the Ning-1 strain was 1.2917, higher than the 1.2298 ratio in the Ning-2 strain (Figure 5C; Table S6), which may affect protein structure and function. These results indicate differences in genetic variation between the two strains, which might be related to their adaptation to various environments or hosts, thereby affecting their biological characteristics and pathogenicity.

Investigation of *Rickettsia aeschlimannii* in ticks

Using SFGR-specific PCR targeting the *ompA* (630 bp), *gltA* (667 bp), *sca1* (777 bp), and *17 kDa* (395 bp) genes, we investigated the prevalence of *R. aeschlimannii* in ticks collected from Shizuishan, Wuzhong, Zhongwei, and Yinchuan in Ningxia, China, during 2022–2023. To ensure accuracy, a sample was considered positive if all four genes tested positive for *R. aeschlimannii*. We identified a total of 99 *R. aeschlimannii*-positive samples among 150 *Hyalomma* ticks, resulting in an overall positive rate of 66.00%. The positive rates were 64.13% for 92 *Hy. asiaticum* and 68.97% for 58 *Hy. scupense*.

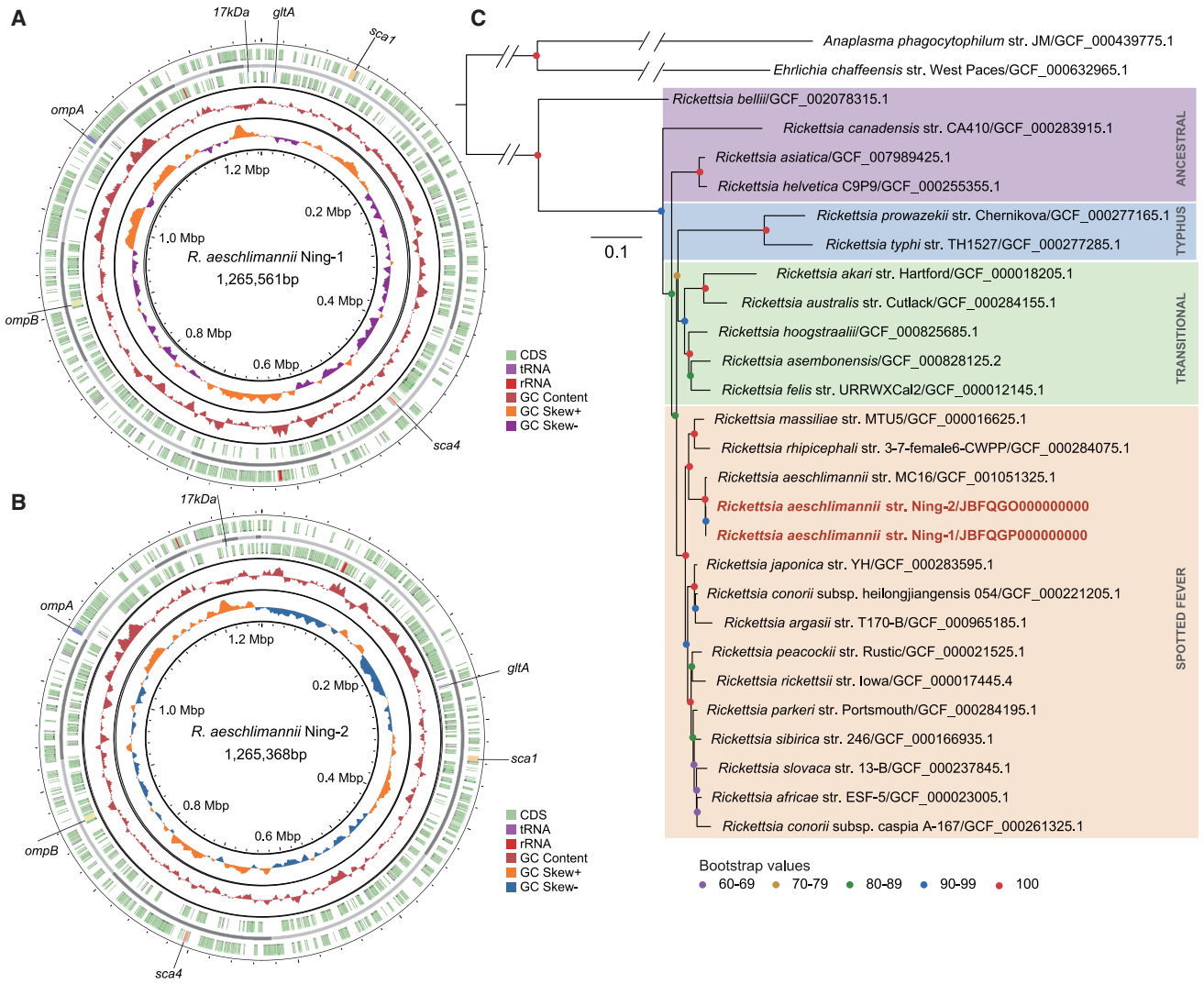

Figure 2. Circular map and phylogenetic tree of two *R. aeschlimannii* strains

(A) Bird's eye view of the assembled genome of *R. aeschlimannii* str. Ning-1.

(B) Bird's eye view of the assembled genome of *R. aeschlimannii* str. Ning-2. From inner circle to outer circle (A and B), the map represents GC skew, GC content, proteins of - strand, contig, and proteins of + strand. The locations of tRNA, rRNA, *ompA*, *ompB*, *gltA*, *17 kDa*, *sca1*, and *sca4* genes within the genome are indicated.

(C) Phylogenetic tree constructed using the maximum likelihood method with 1,000 replications, based on the whole genomes of 26 other publicly available established or proposed Rickettsiales species. *Anaplasma phagocytophilum* and *Ehrlichia chaffeensis* were used as outgroup species to help root the tree. Scale bar indicates 0.1 nucleotide substitutions per site. See also Figure S1.

The sequences of the positive samples have been deposited in GenBank (Table S7).

To further understand the genetic variation and evolutionary positioning of *R. aeschlimannii*, we extracted the *ompA*, *gltA*, *sca1*, and *17 kDa* genes from the three *R. aeschlimannii* genomes to conduct phylogenetic analyses with the sequences of *R. aeschlimannii* available in GenBank (Figure 6). The *ompA* sequences of 99 *R. aeschlimannii* samples shared nucleotide identities ranging from 99.84% to 100% with each other, 99.03%–100% with the Ning-1 and Ning-2 strains, and 98.87%–99.84% with the MC16 strain. The homologies with *R. aeschlimannii* isolates KZQ-B (GenBank: MN794571) and ZDL-3th-NO.6 (GenBank: MW314831), detected in human blood from Xinjiang of China, were 99.78% and 98.18%. Notably, the sequences exhibited 100% homology with *R. aeschlimannii* isolate S11 (GenBank: OR248873) from human blood in Ghana.

The *gltA* sequences obtained in this study demonstrated nucleotide similarity ranging from 99.84% to 100%. The sequences were categorized into two groups based on position 405: one group (58 sequences) was a G at position 405, corresponding to the Ning-1 strain, matching the isolate 420_HB-2017 (GenBank: MT667404) from human blood in Russia. The

Table 1. Genomic characteristics of *Rickettsia aeschlimannii* strains

Characteristic	*R. aeschlimannii* str. Ning-1	*R. aeschlimannii* str. Ning-2	*R. aeschlimannii* str. MC16
Accession ID	JBFQGP000000000	JBFQGO000000000	GCA_001051325.1
Genome size (bp)	1,265,561	1,265,368	1,312,196
BUSCO (%)	99.5 (F:0.0, M:0.5)	99.2 (F:0.3, M:0.5)	99.5 (F:0.0, M:0.5)
GC content (%)	32.21	32.21	32.20
Gene counts	1,500	1,501	1,560
CDS	1,464	1,465	1,524
tRNAs	33	33	33
rRNAs	3	3	3
No. of contigs	11	12	16
N_{50} (bp)	144,368	178,381	210,445
L_{50}	4	4	3
Pseudogene	234	235	248

other group (41 sequences) exhibited a T at position 405, corresponding to the Ning-2 and MC16 strains, and consistent with the isolate RQB050165 (GenBank: KX227762) identified in human blood from Kenya.

In this study, the *17 kDa* and *sca1* sequences from 99 samples exhibited 100% homology, respectively. The *17 kDa* sequences showed 99.00%–99.74% homology with the Ning-1, Ning-2, and MC16 strains, and clustered with sequences reported in various *Hyalomma* tick species worldwide. In contrast, sequences from *Rhipicephalus* and *Haemaphysalis* ticks in Xinjiang, China, as well as those from wild boars in Italy, formed a distinct cluster. These *sca1* sequences showed a homology range of 99.60%–100% with the Ning-1 and Ning-2 strains, and 99.47%–99.87% with MC16 strain. Additionally, they exhibited 99.77%–100% homology with *R. aeschlimannii* isolates KZQ-B and KZQ-U (GenBank: MN733731, MT237576, and MT237577) detected in human blood and urine samples from Xinjiang, China. Consistent with the *17 kDa* sequences, the *sca1* sequences from *Rhipicephalus* and *Haemaphysalis* ticks in Xinjiang also clustered together.

DISCUSSION

This study reports the isolation of two strains of *R. aeschlimannii* from *Hy. scupense* and *Hy. asiaticum* ticks collected in Ningxia, China. These are the strains of pathogenic *Rickettsia* isolated outside the Mediterranean region since their initial discovery in *Hy. marginatum* ticks in 1997. Using next-generation sequencing and *de novo* assembly, we obtained two complete genome sequences of this emerging *Rickettsia*. The study revealed biological differences between the two strains and compared their genomic characteristics and genetic evolution with the Mediterranean strain MC16.

R. aeschlimannii, an emerging tick-borne pathogen initially identified in Mediterranean ticks, is known to cause MSF-like illness. Recently, its geographic range has expanded beyond the Mediterranean, with detections reported in ticks across Africa and Asia.[12,15,16,25,26] This *Rickettsia* has also been detected in ticks parasitizing migratory birds, including *Hyalomma*, *Ixodes*, and *Dermacentor*,[27–29] suggesting that migratory birds may facilitate its spread from Africa to various European countries and potentially to Asia. Multiple human infection cases have been reported outside the Mediterranean,[8,9] highlighting the potential for *R. aeschlimannii* to spread across different regions. Understanding the genetic evolution of *R. aeschlimannii* across different tick species and regions is crucial for preventing its spread and infection.

Although *R. aeschlimannii* has been widely distributed across various regions, only one complete genome sequence from *Hy. marginatum* ticks in Mediterranean countries has been reported to date. In this study, we successfully isolated two strains of *R. aeschlimannii* from two *Hyalomma* species and assembled their complete genome sequences. The Ning-1 and Ning-2 strains consist of circular chromosomes of 1,265,561 bp and 1,265,368 bp, respectively, both smaller than the Mediterranean MC16 strain. Genome reduction is generally associated with increased pathogenicity in *Rickettsia*, with more virulent species often having smaller genomes than their less virulent species.[30] A total of 154 unique orthogroups in the Ning-1 and Ning-2 strains were identified compared to the MC16 strain. Among these homologous genes, 30 are metabolism-related genes across eight categories, suggesting that the two strains may have enhanced metabolic capability compared to the originally identified MC16 strain due to long-term evolution. Virulence gene analysis revealed that both Ning-1 and Ning-2 strains have greater coverage of the *ralF* gene, a type IV secretion system effector, compared to the MC16 strain. The *ralF* gene facilitates *Rickettsia* invasion by activating the host cell's *Arf6* protein to produce phosphoinositide PI (4,5) P2, which is essential for *Rickettsia* entry. Antibody-mediated blockade of *ralF* significantly reduces *Rickettsia* invasion.[24,31] These findings suggest that Ning-1 and Ning-2 strains may exhibit higher virulence compared to the MC16 strain. However, due to the unavailability of the MC16 strain, a direct comparison of their biological characteristics could not be conducted.

Compared to the Ning-2 strain, the Ning-1 strain exhibits a higher growth rate, a more obvious cytopathic effect, and greater plaque formation ability in cell culture infection models. This may be related to its unique gene encoding the *pmp20* protein, which is

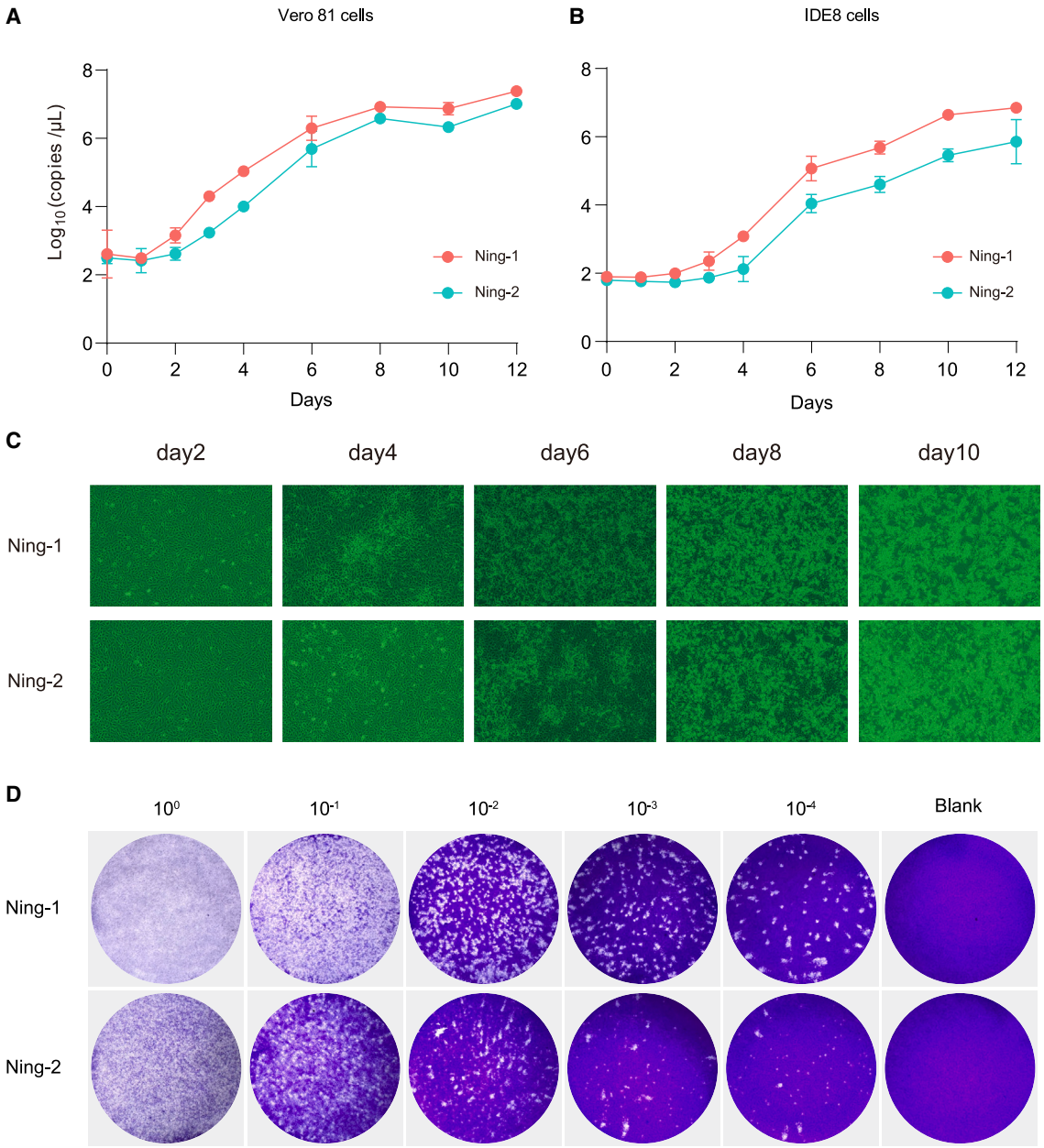

Figure 3. Comparison of growth characteristics between two *R. aeschlimannii* strains

(A) Growth curves of *R. aeschlimannii* str. Ning-1 and *R. aeschlimannii* str. Ning-2 in Vero 81 cells over 288 h.

(B) Growth curves of *R. aeschlimannii* str. Ning-1 and *R. aeschlimannii* str. Ning-2 in IDE8 tick cells over 288 h. Quantitative data from three independent experiments are presented as mean ± SD (shown as error bars) (A and B).

(C) Cytopathic effect in Vero 81 cells induced by the two *R. aeschlimannii* strains.

(D) Plaque formation in Vero 81 cells by the two *R. aeschlimannii* strains with multiple dilutions at 8 days post-infection (dpi).

involved in intracellular trafficking, secretion, and vesicular transport. Although there is no direct evidence indicating that *pmp20* affects the ability of *Rickettsia* to infect cells, *pmp20* has been implicated in mediating the infection of human epithelial cells by *Chlamydia pneumoniae* through its surface short repetitive peptide motifs.[22,23] The Ning-1 strain displays higher frequencies of variants, deletions, transitions, and transversions compared to the Ning-2 strain, and its missense/silent ratio is also higher than that of the Ning-2 strain, which may affect gene expression regulation, protein structure, or function, thus contributing to its enhanced biological characteristics. Future research should focus on elucidating the specific role of the *pmp20* protein in the *Rickettsia* infection process and exploring how SNP variations impact the biological properties and pathogenicity of *Rickettsia*. Additionally,

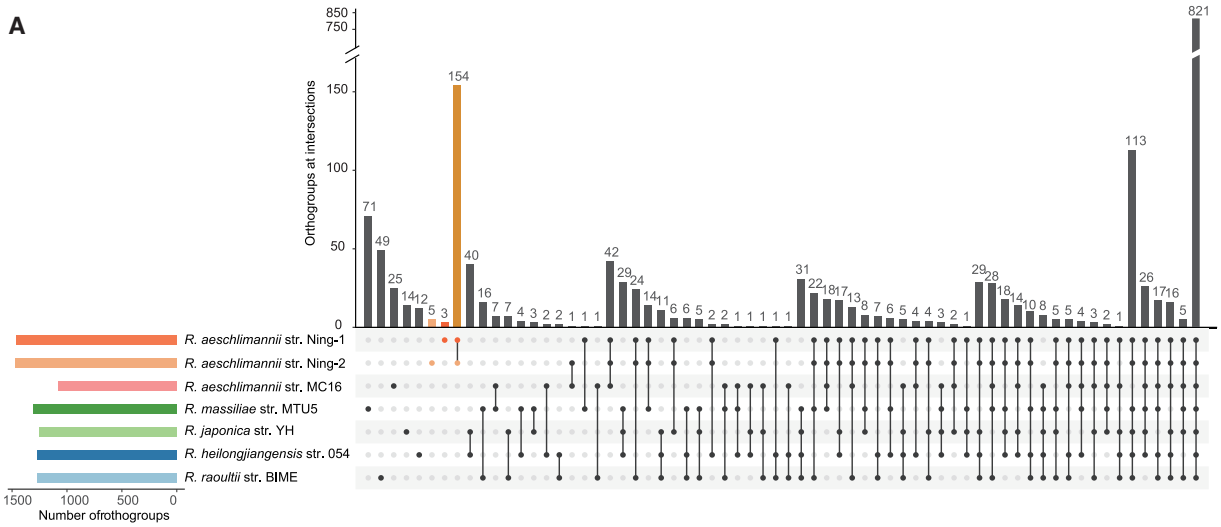

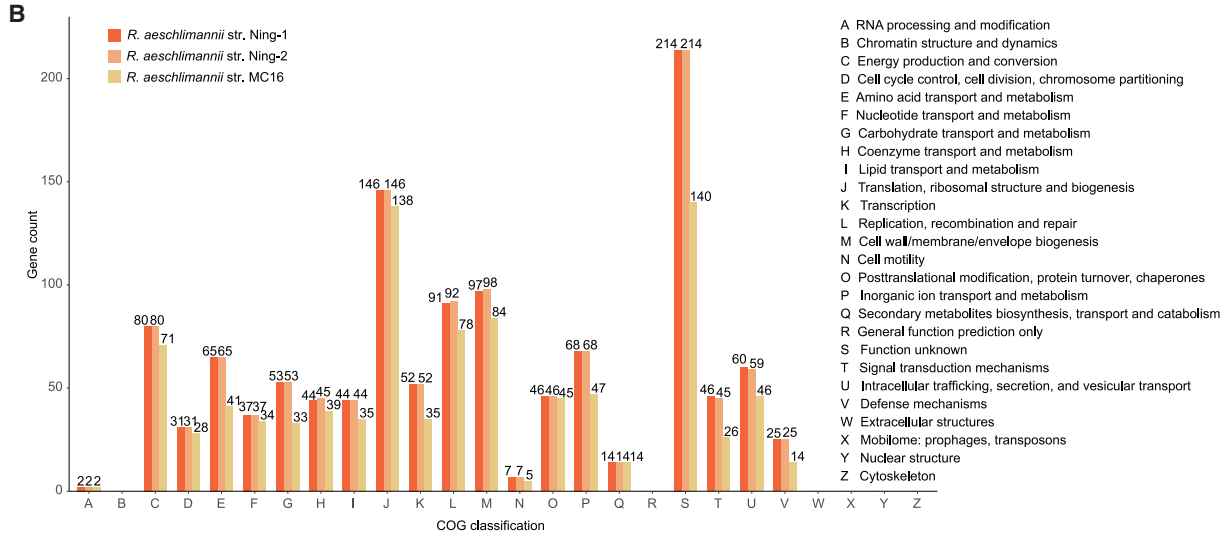

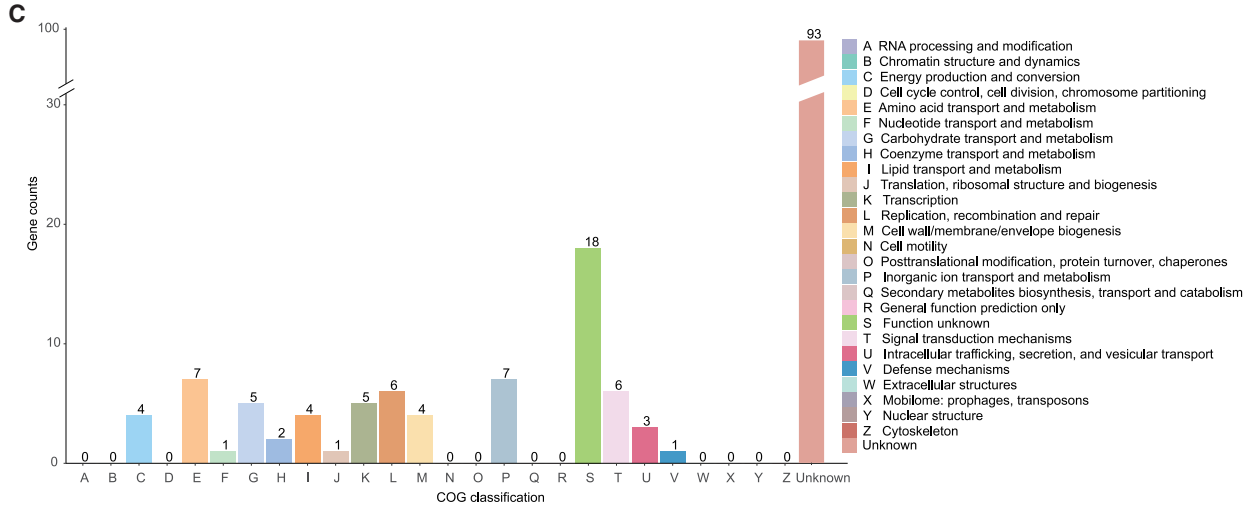

(legend on next page)

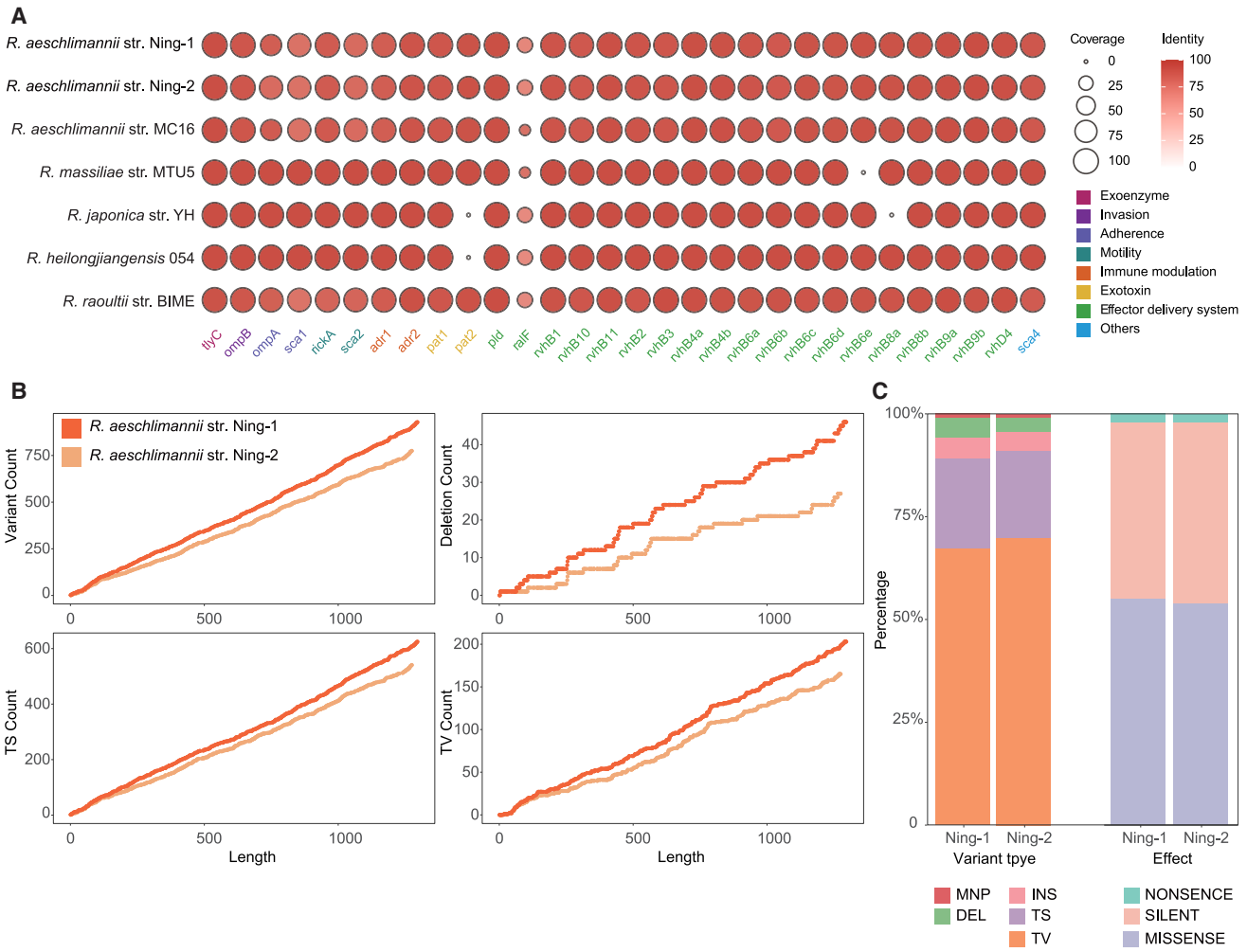

Figure 5. Virulence factors determination and single nucleotide polymorphism analysis of *R. aeschlimannii*

(A) Presence of virulence factors in *R. aeschlimannii* and other representative SFGR genomes. The vertical axis represents various SFGRs, the horizontal axis indicates the names of the virulence factors, the size of the bubbles represents the coverage of the virulence factors, and the color intensity indicates their identity.

(B) Number of variants, deletions, transitions, and transversions of *R. aeschlimannii* strains Ning-1 and Ning-2 with the genome of *R. aeschlimannii* strain MC16 as the reference.

(C) Proportion of total SNPs accounted for by various types and effects of SNPs. See also Tables S4–S6.

the implications of these variations for disease control and vaccine development should be thoroughly examined.

The positive rates of *R. aeschlimannii* in *Hy. asiaticum* and *Hy. scupense* ticks were relatively high, at 64.13% and 68.97%, respectively. Previous studies have reported that the prevalence of *R. aeschlimannii* in *Hy. marginatum* can be as high as 87.3%,[32] and that *R. aeschlimannii* has been isolated from larval *Hyalomma* ticks, suggesting that *Hyalomma* ticks might be the main vectors for its transmission. To date, *R. aeschlimannii* has been detected in 33 different vectors, including 32 tick species,[33] indicating that extensive surveys of ticks and animals are needed to better understand its ecological distribution and transmission.

Overall, we isolated two pathogenic strains of *R. aeschlimannii* from two *Hyalomma* species, compared their biological characteristics, and obtained their complete genomes to elucidate their genetic features through next-generation sequencing. The identification of these two strains with different genetic

Figure 4. Functional annotation of *R. aeschlimannii* genomes

(A) UpsetR plot showing the number of orthogroups in the *R. aeschlimannii* genomes compared with other closely related SFGR representatives. Connected circles indicate shared orthogroups among these SFGR species.

(B) COG annotation of all genes from the three *R. aeschlimannii* strains.

(C) COG annotation of shared homologous genes of Ning-1 and Ning-2 strains. See also Tables S2 and S3.

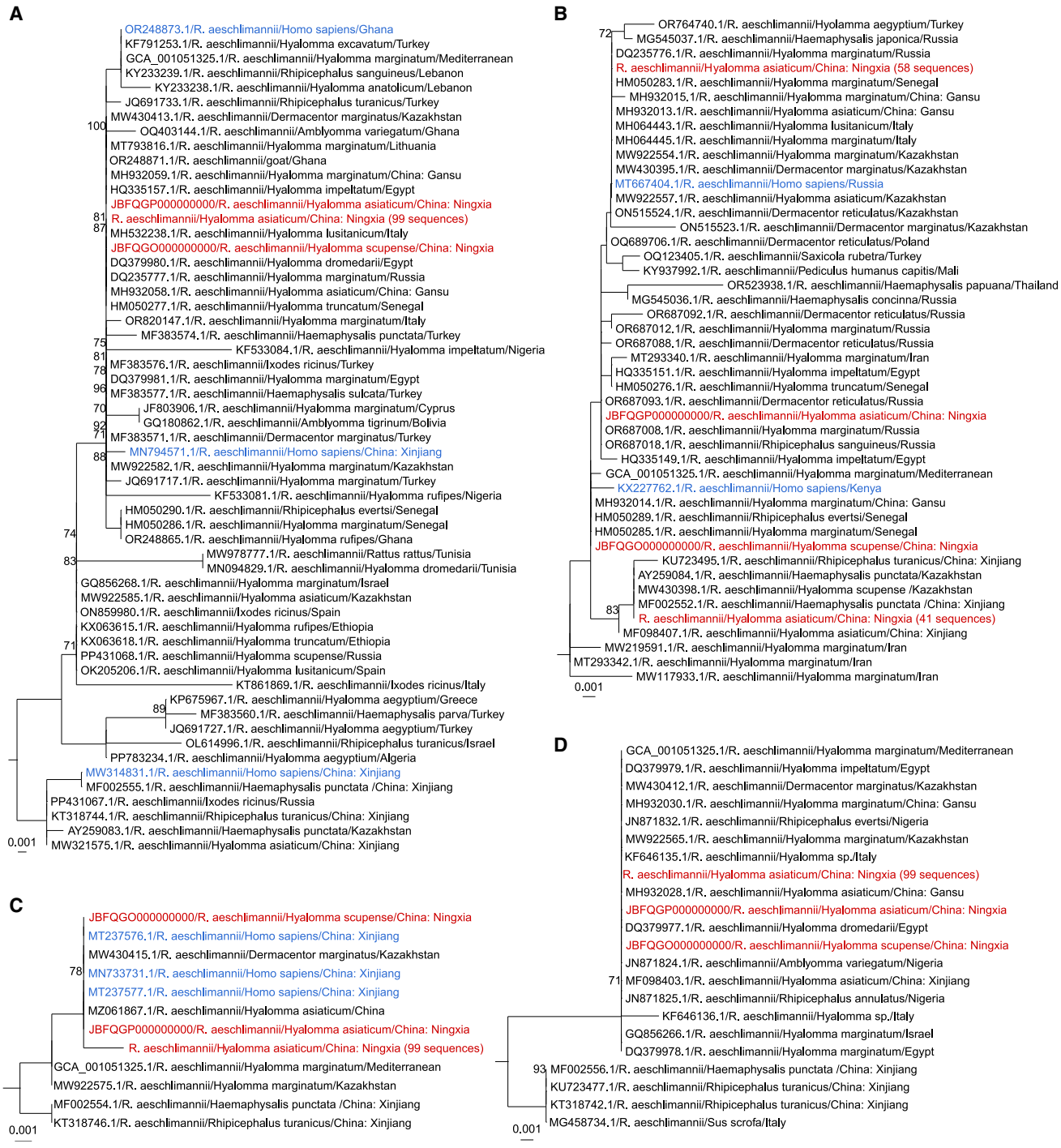

Figure 6. Phylogenetic analysis of *R. aeschlimannii* based on nucleotide sequences of four genes

(A) Phylogenetic tree based on *ompA* gene.

(B) Phylogenetic tree based on *gltA* gene.

(C) Phylogenetic tree based on *sca1* gene.

(D) Phylogenetic tree based on *17 kDa* gene.

(A–D), Bootstrap analysis with 1,000 replicates was conducted to evaluate phylogenetic robustness. Scale bar indicates the number of nucleotide substitutions per site. GenBank accession numbers are provided. Sequences obtained in this study are highlighted in red, while sequences identified from humans are in blue. See also Table S7.

characteristics that differ from the Mediterranean strain emphasizes the critical need for an in-depth understanding of the genetic evolution and biological characteristics of *R. aeschlimannii* across various tick species and geographic regions. Enhanced surveillance in high-risk areas where these tick species are prevalent is vital for the effective prevention and control of this pathogen.

Limitations of the study

A limitation of this study is that it was conducted in a representative area of northwestern China. The geographic distribution and evolutionary characteristics of *R. aeschlimannii* in other regions, such as Xinjiang, remain unclear, which hinders our ability to comprehensively compare strains from different areas. In addition, we should subsequently investigate the prevalence of this *Rickettsia* in tick-bitten patients in the areas with high risks.

RESOURCE AVAILABILITY

Lead contact

Further information and requests for resources and reagents should be directed to and will be fulfilled by the lead contact, Wu-Chun Cao (caowuchun@126.com).

Materials availability

This study did not generate new unique reagents.

Data and code availability

- The genome assembly and genomic DNA sequences generated in this study have been deposited at the National Center for Biotechnology Information (NCBI) and are publicly available as of the date of publication. Accession numbers are listed in the key resources table and the Table S7.
- This paper does not report original code.
- Any additional information required to reanalyze the data reported in this paper is available from the lead contact upon request.

ACKNOWLEDGMENTS

This study was supported by the National Key Research and Development Program of China (2023YFC2305901), the Natural Science Foundation of China (81621005), and the Postdoctoral Fellowship Program and China Postdoctoral Science Foundation (BX20240215).

AUTHOR CONTRIBUTIONS

Conceptualization, W.-C.C.; methodology, N.W.; formal analysis, R.-Z.Y., H.-J.Y., X.-Y.H., L.-F.D., and W.S.; investigation, N.W., D.T., W.-Y.G., B.-H.W., M.-Z.Z., Y.S., L.Z., and X.-M.C.; writing—original draft, N.W.; writing—review and editing, X.-M.C., Z.-H.L., and W.-C.C.; funding acquisition, R.-Z.Y. and W.-C.C.; project administration, X.-Y.S., D.-Y.Z., and J.-F.J.; resources, N.J. and Z.-H.L.; supervision, W.-C.C.

DECLARATION OF INTERESTS

The authors declare no competing interests.

STAR★METHODS

Detailed methods are provided in the online version of this paper and include the following:

SUPPLEMENTAL INFORMATION

Supplemental information can be found online at https://doi.org/10.1016/j.isci.2025.112080.

Received: September 11, 2024
Revised: December 24, 2024
Accepted: February 18, 2025
Published: February 21, 2025

REFERENCES

1. Beati, L., Meskini, M., Thiers, B., and Raoult, D. (1997). *Rickettsia aeschlimannii* sp. nov., a new spotted fever group rickettsia associated with *Hyalomma marginatum* ticks. Int. J. Syst. Bacteriol. *47*, 548–554. https://doi.org/10.1099/00207713-47-2-548.
2. Raoult, D., Fournier, P.E., Abboud, P., and Caron, F. (2002). First documented human *Rickettsia aeschlimannii* infection. Emerg. Infect. Dis. *8*, 748–749. https://doi.org/10.3201/eid0807.010480.
3. Oteo, J.A., and Portillo, A. (2012). Tick-borne rickettsioses in Europe. Ticks Tick. Borne. Dis. *3*, 271–278. https://doi.org/10.1016/j.ttbdis.2012.10.035.
4. Germanakis, A., Chochlakis, D., Angelakis, E., Tselentis, Y., and Psaroulaki, A. (2013). *Rickettsia aeschlimannii* infection in a man, Greece. Emerg. Infect. Dis. *19*, 1176–1177. https://doi.org/10.3201/eid1907.130232.
5. Mokrani, N., Parola, P., Tebbal, S., Dalichaouche, M., Aouati, A., and Raoult, D. (2008). *Rickettsia aeschlimannii* infection, Algeria. Emerg. Infect. Dis. *14*, 1814–1815. https://doi.org/10.3201/eid1411.071221.
6. Mokrani, K., Tebbal, S., Raoult, D., and Fournier, P.E. (2012). Human rickettsioses in the Batna area, eastern Algeria. Ticks Tick. Borne. Dis. *3*, 364–366. https://doi.org/10.1016/j.ttbdis.2012.10.017.
7. Tosoni, A., Mirijello, A., Ciervo, A., Mancini, F., Rezza, G., Damiano, F., Cauda, R., Gasbarrini, A., and Addolorato, G.; Internal Medicine Sepsis Study Group (2016). Human *Rickettsia aeschlimannii* infection: first case with acute hepatitis and review of the literature. Eur. Rev. Med. Pharmacol. Sci. *20*, 2630–2633.
8. Igolkina, Y., Rar, V., Krasnova, E., Filimonova, E., Tikunov, A., Epikhina, T., and Tikunova, N. (2022). Occurrence and clinical manifestations of tick-borne rickettsioses in Western Siberia: first Russian cases of *Rickettsia aeschlimannii* and *Rickettsia slovaca* infections. Ticks Tick. Borne. Dis. *13*, 101927. https://doi.org/10.1016/j.ttbdis.2022.101927.
9. Yang, M., Jia, Y., Dong, Z., Zhang, Y., Xie, S., Liu, Q., and Wang, Y. (2022). *Rickettsia aeschlimannii* Infection in a Woman from Xingjiang, Northwestern China. Vector Borne Zoonotic Dis. *22*, 55–57. https://doi.org/10.1089/vbz.2021.0071.
10. Yin, X., Guo, S., Ding, C., Cao, M., Kawabata, H., Sato, K., Ando, S., Fujita, H., Kawamori, F., Su, H., et al. (2018). Spotted fever group rickettsiae in Inner Mongolia, China, 2015-2016. Emerg. Infect. Dis. *24*, 2105–2107. https://doi.org/10.3201/eid2411.162094.
11. Sadeddine, R., Diarra, A.Z., Laroche, M., Mediannikov, O., Righi, S., Benakhla, A., Dahmana, H., Raoult, D., and Parola, P. (2020). Molecular identification of protozoal and bacterial organisms in domestic animals and

their infesting ticks from north-eastern Algeria. Ticks Tick. Borne. Dis. *11*, 101330. https://doi.org/10.1016/j.ttbdis.2019.101330.

12. Chitimia-Dobler, L., Springer, A., Lang, D., Lindau, A., Fachet, K., Dobler, G., Nijhof, A.M., Strube, C., and Mackenstedt, U. (2024). Molting incidents of *Hyalomma* spp. carrying human pathogens in Germany under different weather conditions. Parasites Vectors *17*, 70. https://doi.org/10.1186/s13071-024-06175-y.
13. Wei, Q.Q., Guo, L.P., Wang, A.D., Mu, L.M., Zhang, K., Chen, C.F., Zhang, W.J., and Wang, Y.Z. (2015). The first detection of *Rickettsia aeschlimannii* and *Rickettsia massiliae* in *Rhipicephalus turanicus* ticks, in northwest China. Parasites Vectors *8*, 631. https://doi.org/10.1186/s13071-015-1242-2.
14. Chisu, V., Leulmi, H., Masala, G., Piredda, M., Foxi, C., and Parola, P. (2017). Detection of *Rickettsia hoogstraalii, Rickettsia helvetica, Rickettsia massiliae, Rickettsia slovaca* and *Rickettsia aeschlimannii* in ticks from Sardinia, Italy. Ticks Tick. Borne. Dis. *8*, 347–352. https://doi.org/10.1016/j.ttbdis.2016.12.007.
15. Boularias, G., Azzag, N., Galon, C., Šimo, L., Boulouis, H.J., and Moutailler, S. (2021). High-throughput microfluidic real-time PCR for the detection of multiple microorganisms in Ixodid cattle ticks in northeast Algeria. Pathogens *10*, 362. https://doi.org/10.3390/pathogens10030362.
16. Igolkina, Y., Rar, V., Vysochina, N., Ivanov, L., Tikunov, A., Pukhovskaya, N., Epikhina, T., Golovljova, I., and Tikunova, N. (2018). Genetic variability of *Rickettsia* spp. in *Dermacentor* and *Haemaphysalis* ticks from the Russian Far East. Ticks Tick. Borne. Dis. *9*, 1594–1603. https://doi.org/10.1016/j.ttbdis.2018.07.015.
17. Majid, A., Almutairi, M.M., Alouffi, A., Tanaka, T., Yen, T.Y., Tsai, K.H., and Ali, A. (2023). First report of spotted fever group *Rickettsia aeschlimannii* in *Hyalomma turanicum, Haemaphysalis bispinosa*, and *Haemaphysalis montgomeryi* infesting domestic animals: updates on the epidemiology of tick-borne *Rickettsia aeschlimannii*. Front. Microbiol. *14*, 1283814. https://doi.org/10.3389/fmicb.2023.1283814.
18. Blanda, V., Torina, A., La Russa, F., D'Agostino, R., Randazzo, K., Scimeca, S., Giudice, E., Caracappa, S., Cascio, A., and de la Fuente, J. (2017). A retrospective study of the characterization of *Rickettsia* species in ticks collected from humans. Ticks Tick. Borne. Dis. *8*, 610–614. https://doi.org/10.1016/j.ttbdis.2017.04.005.
19. Dong, Q., Yang, M., Li, F., Jia, Y., Rizabek, K., Kairullayev, K., Bauyrzhan, O., Adil, K., Oralhazi, K., and Wang, Y. (2023). Spotted fever group rickettsiae in hard ticks in eastern and southern Kazakhstan. Ticks Tick. Borne. Dis. *14*, 102238. https://doi.org/10.1016/j.ttbdis.2023.102238.
20. Orkun, Ö. (2019). Molecular investigation of the natural transovarial transmission of tick-borne pathogens in Turkey. Vet. Parasitol. *273*, 97–104. https://doi.org/10.1016/j.vetpar.2019.08.013.
21. Sentausa, E., El Karkouri, K., Michelle, C., Raoult, D., and Fournier, P.E. (2014). Draft genome sequence of *Rickettsia aeschlimannii*, associated with *Hyalomma marginatum* ticks. Genome Announc. *2*, e00666-14. https://doi.org/10.1128/genomeA.00666-14.
22. Vandahl, B.B., Pedersen, A.S., Gevaert, K., Holm, A., Vandekerckhove, J., Christiansen, G., and Birkelund, S. (2002). The expression, processing and localization of polymorphic membrane proteins in *Chlamydia pneumoniae* strain CWL029. BMC Microbiol. *2*, 36. https://doi.org/10.1186/1471-2180-2-36.
23. Mölleken, K., Schmidt, E., and Hegemann, J.H. (2010). Members of the *Pmp* protein family of *Chlamydia pneumoniae* mediate adhesion to human cells via short repetitive peptide motifs. Mol. Microbiol. *78*, 1004–1017. https://doi.org/10.1111/j.1365-2958.2010.07386.x.
24. Rennoll-Bankert, K.E., Rahman, M.S., Gillespie, J.J., Guillotte, M.L., Kaur, S.J., Lehman, S.S., Beier-Sexton, M., and Azad, A.F. (2015). Which way in? The *ralF* Arf-GEF orchestrates *Rickettsia* host cell invasion. PLoS Pathog. *11*, e1005115. https://doi.org/10.1371/journal.ppat.1005115.
25. Palomar, A.M., Molina, I., Bocanegra, C., Portillo, A., Salvador, F., Moreno, M., and Oteo, J.A. (2022). Old zoonotic agents and novel variants of tick-borne microorganisms from Benguela (Angola), July 2017. Parasites Vectors *15*, 140. https://doi.org/10.1186/s13071-022-05238-2.
26. Paguem, A., Manchang, K., Kamtsap, P., Renz, A., Schaper, S., Dobler, G., Bakkes, D.K., and Chitimia-Dobler, L. (2023). Ticks and Rickettsiae associated with wild animals sold in bush meat markets in Cameroon. Pathogens *12*, 348. https://doi.org/10.3390/pathogens12020348.
27. Wallménius, K., Barboutis, C., Fransson, T., Jaenson, T.G.T., Lindgren, P.E., Nyström, F., Olsen, B., Salaneck, E., and Nilsson, K. (2014). Spotted fever *Rickettsia* species in *Hyalomma* and *Ixodes* ticks infesting migratory birds in the European Mediterranean area. Parasites Vectors *7*, 318. https://doi.org/10.1186/1756-3305-7-318.
28. Pascucci, I., Di Domenico, M., Capobianco Dondona, G., Di Gennaro, A., Polci, A., Capobianco Dondona, A., Mancuso, E., Cammà, C., Savini, G., Cecere, J.G., et al. (2019). Assessing the role of migratory birds in the introduction of ticks and tick-borne pathogens from African countries: An Italian experience. Ticks Tick. Borne. Dis. *10*, 101272. https://doi.org/10.1016/j.ttbdis.2019.101272.
29. Battisti, E., Urach, K., Hodžić, A., Fusani, L., Hufnagl, P., Felsberger, G., Ferroglio, E., and Duscher, G.G. (2020). Zoonotic pathogens in ticks from migratory birds, Italy. Emerg. Infect. Dis. *26*, 2986–2988. https://doi.org/10.3201/eid2612.181686.
30. Merhej, V., and Raoult, D. (2011). Rickettsial evolution in the light of comparative genomics. Biol. Rev. Camb. Phil. Soc. *86*, 379–405. https://doi.org/10.1111/j.1469-185X.2010.00151.x.
31. Rennoll-Bankert, K.E., Rahman, M.S., Guillotte, M.L., Lehman, S.S., Beier-Sexton, M., Gillespie, J.J., and Azad, A.F. (2016). RalF-mediated activation of Arf6 controls *Rickettsia typhi* invasion by co-opting phosphoinositol metabolism. Infect. Immun. *84*, 3496–3506. https://doi.org/10.1128/iai.00638-16.
32. Joly-Kukla, C., Bernard, C., Bru, D., Galon, C., Giupponi, C., Huber, K., Jourdan-Pineau, H., Malandrin, L., Rakotoarivony, I., Riggi, C., et al. (2024). Spatial patterns of *Hyalomma marginatum*-borne pathogens in the Occitanie region (France), a focus on the intriguing dynamics of *Rickettsia aeschlimannii*. Microbiol. Spectr. *12*, e0125624. https://doi.org/10.1128/spectrum.01256-24.
33. Zhang, Y.Y., Sun, Y.Q., Chen, J.J., Teng, A.Y., Wang, T., Li, H., Hay, S.I., Fang, L.Q., Yang, Y., and Liu, W. (2023). Mapping the global distribution of spotted fever group rickettsiae: a systematic review with modelling analysis. Lancet. Digit. Health *5*, e5–e15. https://doi.org/10.1016/s2589-7500(22)00212-6.
34. Roux, V., Fournier, P.E., and Raoult, D. (1996). Differentiation of spotted fever group rickettsiae by sequencing and analysis of restriction fragment length polymorphism of PCR-amplified DNA of the gene encoding the protein rOmpA. J. Clin. Microbiol *34*, 2058–2065. https://doi.org/10.1128/jcm.34.9.2058-2065.1996.
35. Anstead, C.A., and Chilton, N.B. (2013). Detection of a novel *Rickettsia* (Alphaproteobacteria: Rickettsiales) in rotund ticks (*Ixodes kingi*) from Saskatchewan, Canada. Ticks Tick Borne Dis. *4*, 202–206. https://doi.org/10.1016/j.ttbdis.2012.11.013.
36. Du, L.F., Zhang, M.Z., Yuan, T.T., Ni, X.B., Wei, W., Cui, X.M., Wang, N., Xiong, T., Zhang, J., Pan, Y.S., and et al.. (2023). New insights into the impact of microbiome on horizontal and vertical transmission of a tick-borne pathogen. Microbiome *11*, 50. https://doi.org/10.1186/s40168-023-01485-2.
37. Langmead, B., and Salzberg, S.L. (2012). Fast gapped-read alignment with Bowtie 2. Nat. Methods *9*, 357–359. https://doi.org/10.1038/nmeth.1923.
38. Li, H., Handsaker, B., Wysoker, A., Fennell, T., Ruan, J., Homer, N., Marth, G., Abecasis, G., and Durbin, R.; 1000 Genome Project Data Processing Subgroup (2009). The sequence alignment/map format and SAMtools.

Bioinformatics *25*, 2078–2079. https://doi.org/10.1093/bioinformatics/btp352.

39. Bankevich, A., Nurk, S., Antipov, D., Gurevich, A.A., Dvorkin, M., Kulikov, A.S., Lesin, V.M., Nikolenko, S.I., Pham, S., Prjibelski, A.D., et al. (2012). SPAdes: a new genome assembly algorithm and its applications to single-cell sequencing. J. Comput. Biol. *19*, 455–477. https://doi.org/10.1089/cmb.2012.0021.
40. Kang, D.D., Li, F., Kirton, E., Thomas, A., Egan, R., An, H., and Wang, Z. (2019). MetaBAT 2: an adaptive binning algorithm for robust and efficient genome reconstruction from metagenome assemblies. PeerJ *7*, e7359. https://doi.org/10.7717/peerj.7359.
41. Seemann, T. (2014). Prokka: rapid prokaryotic genome annotation. Bioinformatics *30*, 2068–2069. https://doi.org/10.1093/bioinformatics/btu153.
42. Parks, D.H., Imelfort, M., Skennerton, C.T., Hugenholtz, P., and Tyson, G.W. (2015). CheckM: assessing the quality of microbial genomes recovered from isolates, single cells, and metagenomes. Genome Res. *25*, 1043–1055. https://doi.org/10.1101/gr.186072.114.
43. Jain, C., Rodriguez-R, L.M., Phillippy, A.M., Konstantinidis, K.T., and Aluru, S. (2018). High throughput ANI analysis of 90K prokaryotic genomes reveals clear species boundaries. Nat. Commun. *9*, 5114. https://doi.org/10.1038/s41467-018-07641-9.
44. Asnicar, F., Thomas, A.M., Beghini, F., Mengoni, C., Manara, S., Manghi, P., Zhu, Q., Bolzan, M., Cumbo, F., May, U., et al. (2020). Precise phylogenetic analysis of microbial isolates and genomes from metagenomes using PhyloPhlAn 3.0. Nat. Commun. *11*, 2500. https://doi.org/10.1038/s41467-020-16366-7.
45. Minh, B.Q., Schmidt, H.A., Chernomor, O., Schrempf, D., Woodhams, M.D., von Haeseler, A., and Lanfear, R. (2020). IQ-TREE 2: new models and efficient methods for phylogenetic inference in the genomic era. Mol. Biol. Evol. *37*, 1530–1534. https://doi.org/10.1093/molbev/msaa015.
46. McGinnis, S., and Madden, T.L. (2004). BLAST: at the core of a powerful and diverse set of sequence analysis tools. Nucleic Acids Res. *32*, W20–W25. https://doi.org/10.1093/nar/gkh435.
47. Rozewicki, J., Li, S., Amada, K.M., Standley, D.M., and Katoh, K. (2019). MAFFT-DASH: integrated protein sequence and structural alignment. Nucleic Acids Res. *47*, W5–W10. https://doi.org/10.1093/nar/gkz342.
48. Capella-Gutiérrez, S., Silla-Martínez, J.M., and Gabaldón, T. (2009). trimAl: a tool for automated alignment trimming in large-scale phylogenetic analyses. Bioinformatics *25*, 1972–1973. https://doi.org/10.1093/bioinformatics/btp348.
49. Yu, G., Lam, T.T.Y., Zhu, H., and Guan, Y. (2018). Two methods for mapping and visualizing associated data on phylogeny using ggtree. Mol. Biol. Evol. *35*, 3041–3043. https://doi.org/10.1093/molbev/msy194.
50. Emms, D.M., and Kelly, S. (2019). OrthoFinder: phylogenetic orthology inference for comparative genomics. Genome Biol. *20*, 238. https://doi.org/10.1186/s13059-019-1832-y.
51. Conway, J.R., Lex, A., and Gehlenborg, N. (2017). UpSetR: an R package for the visualization of intersecting sets and their properties. Bioinformatics *33*, 2938–2940. https://doi.org/10.1093/bioinformatics/btx364.
52. Cantalapiedra, C.P., Hernández-Plaza, A., Letunic, I., Bork, P., and Huerta-Cepas, J. (2021). EggNOG-mapper v2: functional annotation, orthology assignments, and domain prediction at the metagenomic scale. Mol. Biol. Evol. *38*, 5825–5829. https://doi.org/10.1093/molbev/msab293.
53. Liu, B., Zheng, D., Zhou, S., Chen, L., and Yang, J. (2022). VFDB 2022: a general classification scheme for bacterial virulence factors. Nucleic Acids Res. *50*, D912–D917. https://doi.org/10.1093/nar/gkab1107.
54. Buchfink, B., Reuter, K., and Drost, H.G. (2021). Sensitive protein alignments at tree-of-life scale using DIAMOND. Nat. Methods *18*, 366–368. https://doi.org/10.1038/s41592-021-01101-x.
55. Cingolani, P., Platts, A., Wang, L.L., Coon, M., Nguyen, T., Wang, L., Land, S.J., Lu, X., and Ruden, D.M. (2012). A program for annotating and predicting the effects of single nucleotide polymorphisms, SnpEff: SNPs in the genome of *Drosophila melanogaster* strain w1118; iso-2; iso-3. Fly *6*, 80–92. https://doi.org/10.4161/fly.19695.

STAR★METHODS

KEY RESOURCES TABLE

REAGENT or RESOURCE	SOURCE	IDENTIFIER
Bacterial and virus strains		
Rickettsia aeschlimannii strain Ning-1	This paper	N/A
Rickettsia aeschlimannii strain Ning-2	This paper	N/A
Biological samples		
Hyalomma asiaticum	Collected from Ningxia in 2022–2023, Northwestern China	N/A
Hyalomma scupense	Collected from Ningxia in 2022–2023, Northwestern China	N/A
Chemicals, peptides, and recombinant proteins		
DNase/RNase-Free Water	Solarbio	Cat#R1600
Agarose	Biosharp	Cat#BS081
DL2,000 DNA Marker	Takara	Cat#3427A
Ultra GelRed	Vazyme	Cat#GR501-AA
50×TAE Buffer	Solarbio	Cat#T1060
Water, nuclease-free	Thermo Fisher Technology	Cat#R0581
Dulbecco's Modification Eagle Medium	Gibco	Cat#C11995500BT
Fetal Bovine Serum	Gibco	Cat#A5669701
L15B-300 for ISE6	Hyclone	N/A
Fetal Bovine Serum fo tick cells	ScienCell	Cat#0500
Tryptose phosphate broth	Sigma-Aldrich	Cat#T9157
Lipoprotein Complex	MP Biomedicals	Cat#191476C1
Phosphate buffered saline	Gibco	Cat#C10010500BT
0.25% Trypsin-EDTA (1×)	Gibco	Cat#25200056
0.1% New Germicidal	Lilcon Medical Technologies (Texas)	N/A
75% Ethanol	Lilcon Medical Technologies (Texas)	N/A
Penicillin and Streptomycin	Solarbio	Cat#P1400
Giemsa Staining	Baso	Cat#BA4122
Sucrose-Potassium-Glutamate	This paper	N/A
Low Melting Point Agarose	Invitrogen	Cat#16520050
4% Paraformaldehyde	Meilunbio	Cat#MA0192
Crystal violet	Macklin	Cat#C805211
4% Glu Solution	Servicebio	Cat#G1102
Critical commercial assays		
MiniBEST Viral RNA/DNA Extraction Kit	Takara	Cat#9766
MiniBEST Universal Genomic DNA Extraction Kit	Takara	Cat#9765
PCR Mycoplasma Detection Set	Takara	Cat#6601
DreamTaq Green PCR Master Mix (2×)	Thermo Fisher Technology	Cat#K1081
TB Green® Premix Ex Taq™ (Tli RNaseH Plus)	Takara	Cat#RR420
Deposited data		
Genome of *Rickettsia aeschlimannii* strain Ning-1	This paper	GenBank: JBFQGP000000000
Genome of *Rickettsia aeschlimannii* strain Ning-2	This paper	GenBank: JBFQGO000000000
Genome of *Rickettsia aeschlimannii* strain MC16	GenBank: GCA_001051325.1	https://www.ncbi.nlm.nih.gov/datasets/genome/GCF_001051325.1/

(*Continued on next page*)

Continued

REAGENT or RESOURCE	SOURCE	IDENTIFIER
Genome of *Chlorocebus sabaeus*	GenBank: GCF_015252025.1	https://www.ncbi.nlm.nih.gov/datasets/genome/GCF_015252025.1/
Nucleotide sequences of *Rickettsia aeschlimannii*	This paper	GenBank: PQ122820–PQ123215
Experimental models: Cell lines		
Vero 81 cells	ATCC	Cat#CCL-81
IDE8 cells	Provided by Ulrike Munderloh (University of Minnesota) and the Tick Cell Biobank (University of Liverpool)	N/A
Experimental models: Organisms/strains		
Rickettsia aeschlimannii strain Ning-1	This paper	N/A
Rickettsia aeschlimannii strain Ning-2	This paper	N/A
Oligonucleotides		
ompA: Rr190.70 Forward Primer: ATGGCGAATATTTCTCCAAAA	Roux et al.[34]	N/A
ompA: Rr190.701 Reverse Primer: GTTCCGTTAATGGCAGCATCT	Roux et al.[34]	N/A
gltA: 1-glt1 Forward Primer: GATTGCTTTACTTACGACCC	Igolkina et al.[34]	N/A
gltA: 1-glt2 Reverse Primer: TGCATTTCTTTCCATTGTGC	Igolkina et al.[8]	N/A
gltA: 2-glt3 Forward Primer: TATAGACGGTGATAAAGGAATC	Igolkina et al.[8]	N/A
gltA: 2-glt4 Reverse Primer: CAGAACTACCGATTTCTTTAGC	Igolkina et al.[8]	N/A
sca1: sca159 Forward Primer: CCCGTCTCGTGACTTACC	This paper	N/A
sca1: sca936 Reverse Primer: AGCATTAGGCGATGGTAG	This paper	N/A
17 kDa: 1-17k3 Forward Primer: GCTTTACAAAATTCTAAAAACCATATA	Anstead and Chilton.[35]	N/A
17 kDa: 1-17k5 Reverse Primer: TGTCTATCAATTCACAACTTGCC	Anstead and Chilton.[35]	N/A
17 kDa: 2-Tara17KD13s1 Forward Primer: ATTGTCCGTCAGGTTGGC	Anstead and Chilton.[35]	N/A
17 kDa: 2-Tara17KD408r1 Reverse Primer: CGGGCGGTATGAATAAGC	Anstead and Chilton.[35]	N/A
sca1: Sca1 Forward Primer for qPCR: GTTTGTGGATGCGTGGTA	Du et al.[36]	N/A
sca1: Sca134 Forward Primer for qPCR: AACCCGATAGTAGCAC	Du et al.[36]	N/A
Software and algorithms		
Bowtie2 v2.4.1	Langmead and Salzberg.[37]	http://bowtie-bio.sourceforge.net/bowtie2/index.shtml
SAMtools v1.9	Li et al.[38]	https://www.htslib.org/
SPAdes v3.15.5	Bankevich et al.[39]	https://ablab.github.io/spades
MetaBAT2 v2:2.15	Kang et al.[40]	https://bitbucket.org/berkeleylab/metabat
Prokka v1.13.3	Seemann.[41]	https://github.com/tseemann/prokka
checkM v1.1.3	Parks et al.[42]	https://ecogenomics.github.io/CheckM
fastANI v1.32	Jain et al.[43]	https://github.com/ParBLiSS/FastANI
PhyloPhlAn v3.0.67	Asnicar et al.[44]	https://huttenhower.sph.harvard.edu/phylophlan

(*Continued on next page*)

Continued

REAGENT or RESOURCE	SOURCE	IDENTIFIER
IQ-Tree v2.2.0.3	Minh et al.[45]	https://www.iqtree.org/
Blast+ v2.13.0	McGinnis and Madden.[46]	https://blast.ncbi.nlm.nih.gov/Blast.cgi
MAFFT v7.505	Rozewicki et al.[47]	https://mafft.cbrc.jp/alignment/software/
TrimAl v1.4.rev15	Capella-Gutiérrez et al.[48]	http://trimal.cgenomics.org/
ggtree	Yu et al.[49]	https://yulab-smu.top/ggtree/
GraphPad Prism Software 9.0.0	GraphPad Software	https://www.graphpad.com
ImageView	This paper	N/A
Orthofinder v2.5.4	Emms and Kelly.[50]	https://davidemmslab.github.io/OrthoFinder/
UpsetR	Conway et al.[51]	https://upsetR.ist.ac.at/
EggNOG-mapper v2.1.7	Cantalapiedra et al.[52]	https://eggnog-mapper.embl.de/
Snippy v4.6.0	This paper	https://github.com/tseemann/snippy
VFDB (Virulence Factors of Pathogenic Bacteria)	Liu et al.[53]	https://www.mgc.ac.cn/VFs/main.htm
Diamond v2.1.11	Buchfink et al.[54]	https://github.com/bbuchfink/diamond
SnpEff v5.2	Cingolani et al.[55]	http://snpeff.sourceforge.net/

EXPERIMENTAL MODEL AND STUDY PARTICIPANT DETAILS

Tick collection

Adult *Hy. asiaticum* and *Hy. scupense* ticks were collected from goats in Ningxia, China. Each engorged female tick was individually placed in a 15 mL centrifuge tube to lay eggs, and the ticks were reared under a 12-h light/12-h dark photoperiod at a temperature of 25°C and 95% relative humidity in an artificial climate incubator.

Cell lines

African green monkey kidney Vero 81 cells (ATCC, Cat#CCL-81) were cultured at 37°C and 5% CO_2 in Dulbecco's modified Eagle's medium (DMEM, Gibco, Cat#C11995500BT) containing 10% (v/v) fetal bovine serum (FBS, Gibco, Cat#A5669701). Vero 81 cells were grown in DMEM containing 2% FBS when the cells were used for *Rickettsia* species infection. The *Ixodes scapularis* tick cell line IDE8 was maintained in L15B-300 medium (Hyclone, America) supplemented with 10% tryptose phosphate broth (Sigma-Aldrich, Cat#T9157), 10% FBS (ScienCell, Cat#0500), and 0.1% lipoprotein complex (MP Biomedicals, Cat#191476C1) at 32°C. Vero 81 cells were obtained from ATCC, while IDE8 cell lines were not authenticated. All cell lines were systematically and regularly tested for the absence of mycoplasma contamination with the PCR Mycoplasma Detection Set (Takara, Cat#6601).

METHOD DETAILS

DNA extraction, and PCR screening

DNA was extracted from each pool of larvae (~100 larvae per pool) or adult ticks using the MiniBEST Viral RNA/DNA Extraction Kit (Takara, Cat#9766) following the manufacturer's instructions. *Rickettsia* was then tested using specific PCR assays targeting the *ompA*, *gltA*, *sca1*, and *17 kDa* genes (Table S1), followed by Sanger sequencing to identify the *Rickettsia* species.

Isolation, purification, and DNA extraction of *Rickettsia*

Two pools of *Hy. scupense* and *Hy. asiaticum* larvae were used separately for isolation. The pooled larvae were ground, and the supernatant was inoculated into Vero 81 cells in 24-well culture plates. Giemsa staining and qPCR targeting the *sca1* gene (Table S1) were used to assess the isolation of *Rickettsia* weekly. The culture was harvested from the wells when the cycle threshold (Ct) value was below 15 and then transferred to 25 cm^2 flasks for further proliferation. Once the qPCR Ct value reached 15, we collected the cell culture and blew the cells repeatedly using a 27G needle to release the *Rickettsia*. The mixture was centrifuged at 1,000 ×g for 10 min to remove cell debris. The supernatant was then centrifuged at 17,000 ×g for 10 min at 4°C to enrich the *Rickettsia*. Total DNA was extracted from the purified *Rickettsia* using the MiniBEST Universal Genomic DNA Extraction Kit (Takara, Cat#9765) for next-generation sequencing.

Whole-genome sequencing and assembly

The total DNA was subjected to next-generation sequencing using the RK20208-Rapid Plus DNA Lib Prep Kit for Illumina (ABclonal, China) and the Illumina NovaSeq 6000 platform with paired-end reads (2 × 150 bp). Cleaned reads were mapped to the genome of

Chlorocebus sabaeus (GenBank: GCF_015252025.1) using Bowtie2 v2.4.1 to eliminate the genome of the cell line.[37] The remaining reads were converted to BAM files using SAMtools v1.9.[38] Host-free reads were assembled into contigs using SPAdes v3.15.5.[39] MetaBAT2 v2:2.15 was used for contig binning.[40] Prokka v1.13.3 and checkM v1.1.3 with the lineage_wf argument were used for genome annotation and completeness assessment.[41,42] ANI was estimated using fastANI v1.32.[43]

Phylogenetic analyses

Multiple sequence comparisons based on the whole genome of *R. aeschlimannii* and the genomes of SFGR available in GenBank were performed using PhyloPhlAn v3.0.67.[44] The maximum likelihood phylogenetic tree was constructed using IQ-Tree v2.2.0.3.[45] Furthermore, the *Rickettsia ompA*, *gltA*, *sca1*, and *17 kDa* genes were extracted from the *R. aeschlimannii* genome using Blast+ v2.13.0 after matching with reference genes,[46] combined with Prokka annotation results, and aligned with reference sequences obtained from GenBank using MAFFT v7.505.[47] Poorly aligned parts were trimmed using TrimAl v1.4.rev15.[48] Using *Rickettsia rhipicephalii* as an outgroup, phylogenetic analyses based on four conserved genes were conducted respectively using the maximum likelihood method in IQ-Tree v2.2.0.3. All phylogenetic trees were visualized using the ggtree package in R software.[49]

Growth, cytopathic effect, and plaque assay

Two cell lines were used to compare the growth of two *R. aeschlimannii* strains. Two *R. aeschlimannii* strains (1×10^5 copies/μL) were inoculated onto monolayers of Vero 81 and IDE8 cells in 24-well plates at 32°C for 2 h. After inoculation, the cells were washed, fresh medium was added, and the plates were incubated at 32°C for up to 288 h. At the designated time points, the monolayers were resuspended by scraping. DNA was extracted from 200 μL aliquots of the cell suspensions using the MiniBEST Viral RNA/DNA Extraction Kit. The copy number of *Rickettsia* DNA at each time point was calculated using a standard curve to obtain the growth curve.

The Vero 81 cells were inoculated with *R. aeschlimannii* (1×10^7 copies/μL) in 6-well culture plates and the CPE in the cells were observed on different days post-inoculation under a light microscope (Olympus, Japan). Images were acquired and processed using ImageView software.

Plaque assays were conducted in Vero 81 cells. Briefly, plates were incubated with 5-fold serial dilutions of *R. aeschlimannii* (initial concentration of 1×10^7 copies/μL) onto 6-well plates with Vero 81 cells and incubated at 32°C in a 5% CO_2 atmosphere to observe plaque formation. After incubation for 2 h, each well was washed with phosphate buffered saline (Gibco, Cat#C10010500BT). Each well was then overlaid with 2 mL of DMEM containing 5% FBS and 0.8% low melting point agarose (Invitrogen, Cat#16520050). After solidification, the plates were covered with 1 mL DMEM containing 5% FBS and incubated at 32°C in a 5% CO_2 atmosphere. Subsequently, at the designated time points, the cells were fixed with 4% paraformaldehyde (Meilunbio, Cat#MA0192) for 1 h and stained with 1% crystal violet (Macklin, Cat#C805211) at room temperature for 1 h. The cells were gently washed with water for approximately 5 min to remove agarose and then air-dried before plaque counting.

Functional analysis of predicted genes

Orthofinder v2.5.4 was used to find single-copy ortholog sequences and orthogroups,[50] and UpsetR was used to visualize shared, unique, and intersecting orthogroups.[51] EggNOG-mapper v2.1.7 was employed for function annotation of the *R. aeschlimannii* genome and selected reference genomes in GenBank.[52] The functions of predicted protein-coding sequences (CDSs) were identified by searching against COG and eggNOG. This analysis used an E-value threshold of $1e^{-5}$ and was followed by filtering to retain only the best matches.

Virulence gene analysis

The full database (setB) of predicted virulence factor data and annotation files were downloaded from the VFDB database.[53] Diamond v2.1.11 was used to align the protein sequences of *R. aeschlimannii* against the virulence gene database.[54] The alignment results were filtered to retain only those virulence genes that belonged to the *Rickettsia* genus category. The identity and coverage were calculated based on the length of the aligned sequences.

Single nucleotide polymorphism assay

Snippy v4.6.0 (https://github.com/tseemann/snippy) was used to identify variant sites in the study genomes relative to the reference genome. The VCF files describing the variant sites were then input into SnpEff v5.2 to analyze variant types and mutation effects.[55]

QUANTIFICATION AND STATISTICAL ANALYSIS

Data processing of the growth curves of two *R. aeschlimannii* strains was performed using GraphPad version Prism 9.0.0 software for statistical analysis (Figure 3A). Data were presented as mean ± SD (shown as error bars) at each time point and were analyzed for statistical significance by the two-sided Student's t test to compare two independent groups.